Two Efficient Procedures to Correct the Positioning Errors in the Plane-Polar Scanning

Francesco D'Agostino, Flaminio Ferrara, Claudio Gennarelli *, Rocco Guerriero, Massimo Migliozzi

D.I.In. - Università di Salerno, via Giovanni Paolo II, 132 - 84084 Fisciano, Italy
*cgennarelli@unisa.it

Abstract: Two techniques to effectively compensate known positioning errors in a plane-polar near field - far field (NF–FF) transformation, using a minimum number of NF data and adopting an oblate ellipsoid to shape the considered antenna, are proposed and validated through experimental proofs. The former makes use of the singular value decomposition method to recover the voltage samples which would be acquired by the probe at the points fixed by the nonredundant sampling representation from the collected positioning error affected ones, whereas the latter employs an iterative scheme. The NF data required by the classical NF–FF transformation with plane-rectangular scanning are then efficiently evaluated via a two-dimensional optimal sampling interpolation formula. The effectiveness of the proposed techniques is assessed by experimental tests performed at the UNISA Antenna Characterization Lab.

1. Introduction

The request for precise measurements of the antenna radiated far field is increased more and more in the last decades due to the growing use of high-performance antennas commonly adopted in new generation radar systems and satellite communication links. On the other hand, these accurate measurements can be performed only in an anechoic chamber, which suitably reproduces the free-space propagation, by almost completely removing the field reflected from the walls. In any case, high-performance antennas are usually electrically large so that in practice only their radiated near field can be measured in an anechoic chamber. Accordingly, the antenna far field must be recovered from the acquired near-field data by applying near-field – far-field (NF–FF) transformation techniques [1-5]. When dealing with directive antennas characterized by pencil beam patterns, the standard plane-rectangular NF–FF transformation [6] can be conveniently employed. A more suitable alternative to such a scanning [7-16] is the plane-polar one (Fig. 1), which can be accomplished through a linear displacement of the probe and a rotational movement of the antenna, thus resulting mechanically simpler than the plane-rectangular one. Moreover, it allows one to acquire the NF data on a greater measurement area with respect to that available in a plane-rectangular NF facility for a given size of the chamber, as well as to measure gravitationally sensitive spaceborne antennas, which can be positioned pointing skyward. In the earliest approach [7, 8], the plane-polar NF–FF transformation was accomplished by employing a Jacobi-Bessel expansion to recover the antenna FF pattern, which required a large computer time. Such a shortcoming has been overcome in [9] by applying a very simple bivariate Lagrange interpolation formula to reconstruct the NF data needed by the plane-rectangular

NF–FF transformation from those taken through the plane-polar scanning, thus allowing the efficient FF pattern reconstruction by means of the fast Fourier transform (FFT) algorithm. A more efficient interpolation scheme has been developed in [10]. It relies on the spatial bandlimitation properties of radiated electromagnetic (EM) fields [17] and employs the optimal sampling interpolation (OSI) expansions of central type, which minimize the truncation error for a given number of retained nearest samples. Although a remarkably reduced number of data with respect to the approaches [7-9, 11, 12] is required, this number is still unbounded when the scanning area approaches infinity. Efficient sampling representations on a plane using a minimum number of NF data collected through a plane-polar facility, which results to be finite also when the measurement area is unbounded, have been developed by properly exploiting the nonredundant sampling representations of the EM fields [18, 19] and considering the antenna under test (AUT) as enclosed either in a double bowl [13, 14] or in an oblate ellipsoid [15, 16]. A considerable saving of the required NF data and corresponding measurement time is so achieved.

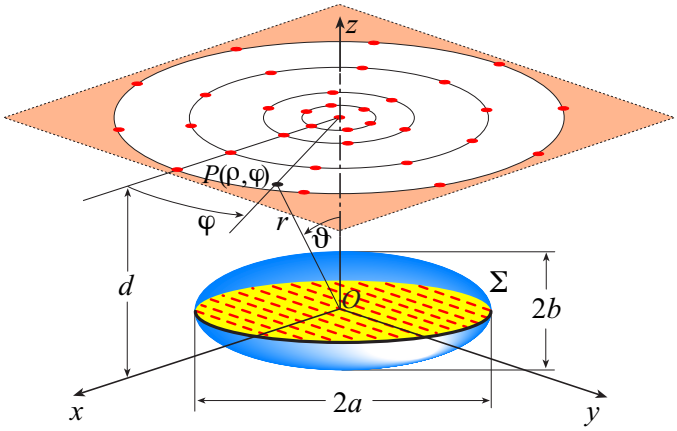

Fig. 1. *Plane-polar scan: dots specify the positions of the nonredundant sampling points on the measurement rings*

The finite resolution of the positioners, as well as their imprecise control, may preclude the exact positioning of the probe at the specified sampling points, even though optical tools can be used to exactly determine their position. Accordingly, it becomes of crucial importance to develop an efficient algorithm for an accurate and stable reconstruction of the required plane-rectangular NF data from the collected irregularly spaced (nonuniform) ones. To this end, the use of the conjugate gradient iteration method together with the unequally spaced FFT [20] has been proposed to compensate known positioning errors in the standard plane-rectangular NF–FF transformation [21]. However, such an approach is not tailored for the nonredundant plane-polar NF–FF transformation techniques [13-16]. As suggested in [22], a more suitable approach is to recover the regularly distributed (uniform) samples from the nonuniform ones and then evaluate the required NF data through a precise and robust OSI expansion. To this end, two diverse procedures have been developed. The former makes use of an iterative scheme converging when a one-to-

one correspondence between each uniform sampling point and the nearest nonuniform one occurs and has been used in [22, 23] for reconstructing plane-rectangular, cylindrical and spherical regularly spaced samples. The latter, employing the singular value decomposition (SVD) method, does not show such a constraint and has been exploited in the plane-polar [24] and cylindrical [25] scannings. However, it can be profitably employed only when the retrieval of the uniform samples can be factorized in two independent one-dimensional problems, otherwise a considerable computational effort is required due to the large sizes of the involved matrix. These techniques have been assessed from the experimental viewpoint in [26, 27] with reference to the cylindrical scanning. Finally, they have been properly extended in [28] to the compensation of positioning errors in the nonredundant spherical NF–FF transformation for elongated antennas employing a prolate ellipsoidal AUT modelling.

The aim of this paper is to properly extend the application of these techniques to the compensation of known positioning errors in the nonredundant plane-polar NF–FF transformation [15, 16] adopting an oblate ellipsoid to shape an antenna and to provide their experimental assessment.

2. Nonredundant representation on a plane

A nonredundant sampling representation of the voltage acquired by a nondirective probe on a plane at distance d by a quasi-planar AUT and the corresponding OSI expansion are briefly recalled in this section. The spherical coordinate system (r, ϑ, φ) is adopted to denote an observation point P and the AUT is considered as enclosed in an oblate ellipsoid Σ, having semimajor and semiminor axes equal to a and b, respectively (Fig. 1). According to [18, 19], it is convenient to introduce the "reduced voltage"

$$\tilde{V}(\xi) = V(\xi)\, \mathrm{e}^{\mathrm{j}\gamma(\xi)} \tag{1}$$

where ξ is an optimal parameter to be used for describing either the radial lines or the rings representing the plane, $\gamma(\xi)$ is a suitable phase function, and $V(\xi)$ is the voltage acquired by the probe (V_φ) or by the rotated probe (V_ρ), (ρ,φ) being the plane-polar coordinates. The error resulting when $\tilde{V}(\xi)$ is approximated by a bandlimited function can be effectively reduced by imposing that this function has a properly increased bandwidth $\chi' W_\xi$, W_ξ being a critical value and $\chi' > 1$ the bandwidth enlargement factor [18].

For a radial line, it results [15, 18]:

$$W_\xi = (2\beta a/\pi)\, E(\pi/2 | \varepsilon^2) \tag{2}$$

$$\xi = (\pi/2) \left[E\left(\sin^{-1} u | \varepsilon^2\right) \big/ E\left(\pi/2 | \varepsilon^2\right) \right] \tag{3}$$

$$\gamma = \beta a\left[v\sqrt{\frac{v^2-1}{v^2-\varepsilon^2}} - E\left(\cos^{-1}\sqrt{\frac{1-\varepsilon^2}{v^2-\varepsilon^2}} \,\middle|\, \varepsilon^2 \right)\right] \tag{4}$$

where $E(\bullet \mid \bullet)$ is the elliptic integral of second kind, β is the free-space wavenumber, $u = (r_1 - r_2)/2f$ and $v = (r_1 + r_2)/2a$ are the elliptic coordinates, $r_{1,2}$ being the distances between the observation point P and the foci of the ellipse C' (intersection between Σ and a meridian plane), f is its semi-interfocal distance, and $\varepsilon = f/a$ the eccentricity.

On a ring, the phase function γ is constant and the angle φ can be conveniently chosen as optimal parameter. The corresponding bandwidth is $W_\varphi(\xi) = \beta a \sin\vartheta_\infty(\xi)$ [15, 18], wherein $\vartheta_\infty = \sin^{-1}u$ is the polar angle of the asymptote to the hyperbola at $\xi = \text{const}$ through P.

According to the above results, the voltage at the observation point P on the radial line at φ can be reconstructed by the OSI expansion [15, 16]:

$$V(\xi(\vartheta),\varphi) = \mathrm{e}^{-\mathrm{j}\gamma(\xi)} \sum_{n=n_0-q+1}^{n_0+q} \tilde{V}(\xi_n,\varphi)\, G\left(\xi,\xi_n,\bar{\xi},N,N''\right) \tag{5}$$

where $n_0 = n_0(\xi) = \mathrm{Int}(\xi/\Delta\xi)$, $2q$ is the number of retained intermediate samples $\tilde{V}(\xi_n,\varphi)$, namely, the reduced voltages at the points corresponding to the intersections between the radial line and the sampling rings,

$$\xi_n = n\Delta\xi = 2\pi n/(2N''+1); \qquad N'' = \mathrm{Int}(\chi N') + 1 \tag{6}$$

$$N' = \mathrm{Int}\left(\chi' W_\xi\right) + 1; \qquad N = N'' - N'; \qquad \bar{\xi} = q\Delta\xi \tag{7}$$

Int(x) denotes the integer part of x, $\chi > 1$ is the oversampling factor needed to control the truncation error [18], and

$$G\left(\xi,\xi_n,\bar{\xi},N,N''\right) = \Omega_N\left(\xi-\xi_n,\bar{\xi}\right) D_{N''}(\xi-\xi_n) \tag{8}$$

Moreover,

$$D_{N''}(\xi) = \frac{\sin[(2N''+1)\xi/2]}{(2N''+1)\sin(\xi/2)} \tag{9}$$

$$\Omega_N\left(\xi,\bar{\xi}\right) = \frac{T_N\left[2\cos^2(\xi/2)/\cos^2\left(\bar{\xi}/2\right)-1\right]}{T_N\left[2/\cos^2\left(\bar{\xi}/2\right)-1\right]} \tag{10}$$

are the Dirichlet and Tschebyscheff sampling functions [18], $T_N(\xi)$ being the Tschebyscheff polynomial

of degree N.

The intermediate samples can be determined by interpolating the samples on the rings through the OSI formula [15, 16]:

$$\tilde{V}(\xi_n,\varphi) = \sum_{m=m_0-p+1}^{m_0+p} \tilde{V}(\xi_n,\varphi_{m,n})\, G(\varphi,\varphi_{m,n},\overline{\varphi},M_n,M_n'') \tag{11}$$

where $m_0 = m_0(\varphi) = \mathrm{Int}(\varphi/\Delta\varphi_n)$, $2p$ is the number of considered nearest reduced voltage samples $\tilde{V}(\xi_n,\varphi_{m,n})$ on the ring specified by ξ_n, and

$$\varphi_{m,n} = m\Delta\varphi_n = 2\pi m/(2M_n''+1)\ ; \qquad M_n'' = \mathrm{Int}(\chi\, M_n')+1 \tag{12}$$

$$M_n' = \mathrm{Int}\left[\chi^* W_\varphi(\xi_n)\right]+1\ ; \qquad M_n = M_n'' - M_n' \tag{13}$$

$$\chi^* = 1+(\chi'-1)[\sin\vartheta_\infty(\xi_n)]^{-2/3}\ ; \qquad \overline{\varphi} = p\Delta\varphi_n \tag{14}$$

By matching (5) and (11), it is possible to accurately reconstruct the voltages V_φ and V_ρ, which would be measured by the probe and rotated probe, at the points needed by the plane-rectangular NF–FF transformation [6]. Unfortunately, the probe corrected formulas in [6] (whose expressions in the here adopted reference system can be found in [29]) are valid as long as the probe maintains its orientation with respect to the AUT and this requires its co-rotation with it. This can be avoided by using a probe exhibiting only a first-order azimuthal dependence in its radiated far field, as, f.i., an open-ended rectangular waveguide excited by a TE_{10} mode [30]. In fact, in such a case, the voltages V_V and V_H (measured by the probe and rotated probe with co-rotation) can be determined from V_φ and V_ρ via the relations:

$$V_V = V_\varphi\cos\varphi - V_\rho\sin\varphi\ ; \qquad V_H = V_\varphi\sin\varphi + V_\rho\cos\varphi \tag{15}$$

3. Uniform samples retrieval

Two efficient procedures to compensate known positioning errors are developed in this section by highlighting their respective advantages and shortcomings.

3.1. The SVD technique

It is assumed that, except the sample at the pole $\vartheta = 0$, all the other are irregularly spaced on rings not uniformly distributed on the scanning plane. This is a realistic hypothesis in a plane-polar NF facility, when the NF data are acquired by moving along rings as required to exploit the possibility to reduce the num-

ber of NF data on the noncentral rings, offered by the previous nonredundant representation. In such a case, the uniform samples reconstruction can be reduced to the solution of two independent one-dimensional problems.

The uniform $2M_k'' + 1$ samples on a nonuniform ring at $\vartheta(\eta_k)$ are recovered as described in the following. Given a sequence of $J_k \geq 2M_k'' + 1$ nonuniform sampling points (η_k, ϕ_j) on such a ring, the related voltages $\tilde{V}(\eta_k, \phi_j)$ can be rewritten as function of the uniform samples through expansion (11), thus obtaining a linear system that can be expressed in the matrix form $\underline{\underline{A}}\,\underline{x} = \underline{b}$, where $\underline{b}$ is the vector of known nonuniform samples $\tilde{V}(\eta_k, \phi_j)$, $\underline{x}$ is that of the unknown uniform ones $\tilde{V}(\eta_k, \varphi_{m,k})$, and $\underline{\underline{A}}$ is a $J_k \times (2M_k'' + 1)$ matrix, whose elements are:

$$a_{jm} = G\left(\phi_j, \varphi_{m,k}, \overline{\varphi}_k, M_k, M_k''\right) \tag{16}$$

where $\varphi_{m,k} = m\Delta\varphi_k = 2m\pi/(2M_k'' + 1)$ and $\overline{\varphi}_k = p\Delta\varphi_k$. Note that, for a fixed row j, the elements a_{jm} are zero if the index m is external to the range $[m_0(\phi_j) - p + 1, m_0(\phi_j) + p]$. The SVD method is then employed to obtain the best least square approximated solution of the system. After this step, the OSI expansion (11), wherein the samples $\tilde{V}(\eta_k, \varphi_{m,k})$ take the role of the $\tilde{V}(\xi_n, \varphi_{m,n})$ ones, is used to determine the intermediate samples $\tilde{V}(\eta_k, \varphi)$ at the intersection points between the nonuniform rings and the radial line through P. Since these samples are again nonuniform, the voltage at P can be found by retrieving the uniform intermediate samples $\tilde{V}(\xi_n, \varphi)$ again via SVD and then interpolating them by means of (5).

Both the distances between each nonuniform ring and the related uniform one and those between the nonuniform sampling points and the associated uniform ones on the nonuniform rings have been assumed less than one half of the corresponding uniform spacing to avoid a strong ill-conditioning of the related linear system. Moreover, the same number N_φ of uniform samples (that corresponding to the largest uniform ring) has been retrieved on each nonuniform ring to minimize the computational effort. In fact, in such a case, the samples are aligned along the radial lines and, therefore, the number of systems to be solved is minimum.

Once the uniform samples have been recovered, the voltages V_φ and V_ρ at the points needed by the plane-rectangular NF–FF transformation [6] can be determined by means of expansions (5) and (11), this last properly modified to account for the redundancy in φ.

3.2. The iterative technique

It is assumed that, save for the sample at the pole $\vartheta = 0$, all the others are irregularly spaced on the scan plane and no longer lie on rings. Moreover, it is also assumed that their distribution is such that there is a one-to-one correspondence between each uniform sampling point and the nearest nonuniform one. In such a case, the SVD-based approach could be still used, but the dimension of the involved matrix would become very large, thus requiring a large computational effort. Accordingly, in such a case, it is more convenient [26-28] to resort to the iterative technique. By expressing the reduced voltages at each nonuniform sampling point $(\eta_k, \phi_{j,k})$ as function of the unknown uniform samples $\tilde{V}(\xi_n, \varphi_{m,n})$ by means of expansions (5) and (11), the following linear system results:

$$\tilde{V}(\eta_k, \phi_{j,k}) = \sum_{n=n_0-q+1}^{n_0+q} \left\{ G\left(\eta_k, \xi_n, \overline{\xi}, N, N''\right) \sum_{m=m_0-p+1}^{m_0+p} \tilde{V}(\xi_n, \varphi_{m,n}) G\left(\phi_{j,k}, \varphi_{m,n}, \overline{\varphi}, M_n, M_n''\right) \right\} \tag{17}$$

It can be recast in the matrix form $\underline{\underline{A}}\,\underline{x} = \underline{b}$, where $\underline{\underline{A}}$ is a $Q \times Q$ sparse matrix, Q being the total number of nonuniform/uniform sampling points, whereas $\underline{x}$ and $\underline{b}$ are the vectors of the unknown uniform and known nonuniform samples, respectively. By subdividing $\underline{\underline{A}}$ into its diagonal $\underline{\underline{A}}_D$ and nondiagonal $\underline{\underline{\Delta}}$ components, multiplying by $\underline{\underline{A}}_D^{-1}$ the system $\underline{\underline{A}}\,\underline{x} = \underline{b}$, and finally rearranging its terms, the following iterative scheme results:

$$\underline{x}^{(\nu)} = \underline{\underline{A}}_D^{-1}\underline{b} - \underline{\underline{A}}_D^{-1}\,\underline{\underline{\Delta}}\;\underline{x}^{(\nu-1)} = \underline{x}^{(0)} - \underline{\underline{A}}_D^{-1}\,\underline{\underline{\Delta}}\;\underline{x}^{(\nu-1)} \tag{18}$$

$\underline{x}^{(\nu)}$ being the vector of the uniform samples estimated at the νth step. It is worth noting that, for the assumed hypothesis about the distribution of the nonuniform samples, each element on the principal diagonal of $\underline{\underline{A}}$ is non-zero and has an amplitude greater than those of the other elements of the same column and row, so that the necessary conditions [22] for the iterative algorithm convergence are fulfilled. By making explicit rel. (18), it results:

$$\tilde{V}^{(\nu)}(\xi_n, \varphi_{m,n}) = \frac{1}{G\left(\eta_n, \xi_n, \overline{\xi}, N, N''\right) G\left(\phi_{m,n}, \varphi_{m,n}, \overline{\varphi}, M_n, M_n''\right)}$$

$$\times \left\{ \tilde{V}(\eta_n, \phi_{m,n}) - \sum_{\substack{\ell=\ell_0-q+1 \\ (\ell \neq n) \wedge (i \neq m)}}^{\ell_0+q} \sum_{i=i_0-p+1}^{i_0+p} G\left(\eta_n, \xi_\ell, \overline{\xi}, N, N''\right) \right.$$

$$\times G\left(\phi_{m,n},\varphi_{i,\ell},\overline{\varphi},M_\ell,M_\ell''\right)\tilde{V}^{(\nu-1)}(\xi_\ell,\varphi_{i,\ell})\Big\} \tag{19}$$

Then, the voltages V_φ and V_ρ at the points required by the NF–FF transformation with plane-rectangular scan [6] can be accurately reconstructed by applying the OSI expansions (5) and (11).

4. Experimental assessment

The described procedures for correcting the positioning errors have been experimentally assessed in the anechoic chamber of the Antenna Characterization Lab of the University of Salerno, wherein a versatile NF facility implementing the plane-polar scanning besides the cylindrical and the spherical ones (see Fig. 2) is available. In particular, the plane-polar scanning is accomplished by mounting the AUT on the rotator performing the φ angle scan and the probe (an open-ended WR90 rectangular waveguide) on the linear vertical positioner. A vector network analyzer is employed to perform the amplitude and phase measurements. The considered AUT is a H-plane monopulse antenna, located in the plane $z = 0$ and working in the sum mode at 10 GHz. It has been made by using a hybrid Tee and two pyramidal horns, whose apertures (8.9×6.8 cm sized) are at a distance of 26 cm (between centers). Such an AUT has been modelled by an oblate ellipsoid with $a = 18.3$ cm and $b = 6.6$ cm. Moreover, $\chi' = 1.35$ and $\chi = 1.20$ have been employed in the sampling representation. The irregularly spaced samples have been collected on a circle of radius 110 cm on a plane, which is located at 17.0 cm from the antenna.

The first set of results (from Fig. 3 to Fig. 8) is relevant to the case of the irregularly spaced sampling points lying on rings. The acquired NF data are such that the distances from each nonuniform ring to the corresponding uniform one, as well as those from the nonuniform sampling points to the associated uniform ones on the rings are random variables having a uniform distribution in $[-\Delta\xi/2,\Delta\xi/2]$ and $[-\Delta\varphi_k/2,\ \Delta\varphi_k/2]$, respectively. The amplitude and phase of V_φ on the radial line at $\varphi = 0°$, obtained via the SVD approach, are compared in Figs. 3 and 4 with the directly measured ones. The reconstructions of the amplitudes of V_φ and V_ρ on the radial line at $\varphi = 30°$ are reported in Fig. 5, whereas that relevant to the phase of V_φ is shown in Fig. 6. As can be seen, in spite of the severe values of the considered positioning errors, all reconstructions result very accurate, save for the peripheral zones with very low voltage levels (below about –60 dB), wherein the error is mainly due to the noise and to the residual reflections from the anechoic chamber walls. Moreover, the recovered voltages exhibit a smoother behaviour with respect to the measured ones, since the spectral content of the noise at the spatial frequencies higher than the antenna

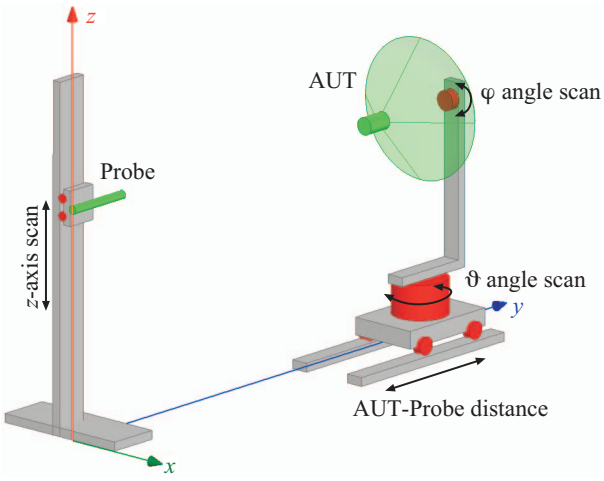

***Fig.** 2 . Sketch of the versatile NF facility available at the Antenna Characterization Lab of the University of Salerno*

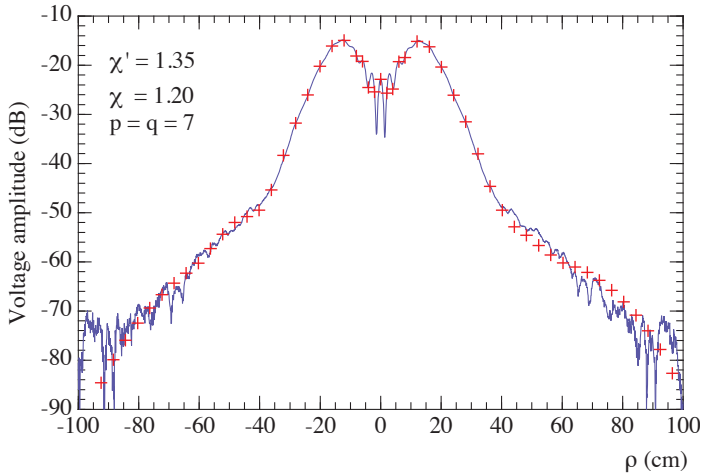

***Fig.** 3 . Amplitude of V_φ along the radial line at $\varphi = 0°$. Solid line: measured. Crosses: retrieved from the irregularly spaced NF data through the SVD-based technique.*

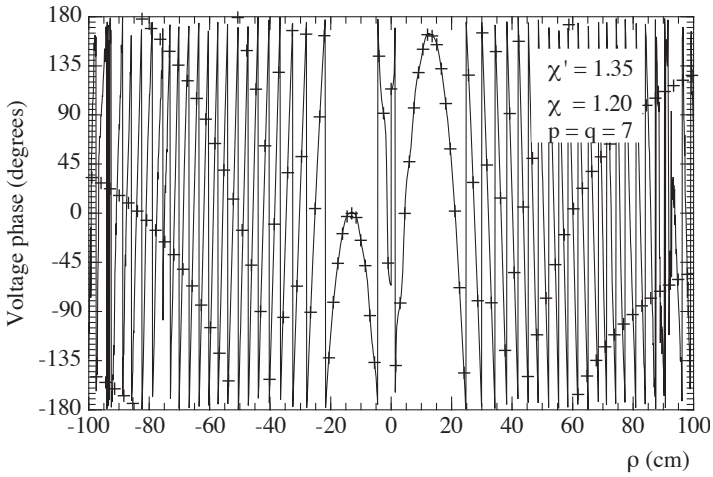

***Fig.** 4. Phase of V_φ along the radial line at $\varphi = 0°$. Solid line: measured. Crosses: retrieved from the irregularly spaced NF data through the SVD-based technique.*

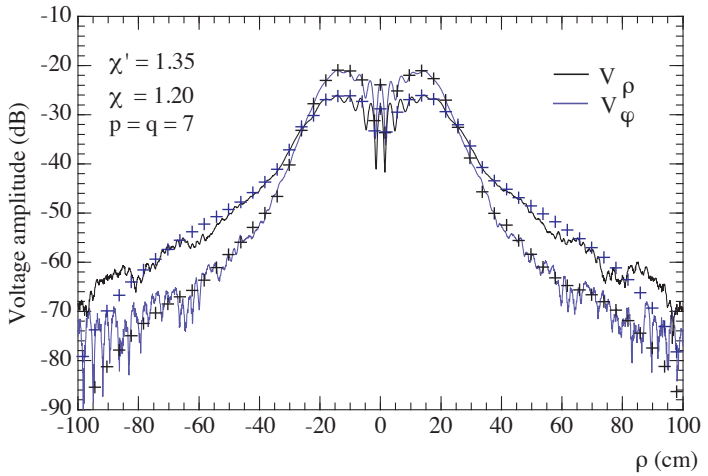

Fig. 5. *Amplitudes of V_φ, V_ρ along the radial line at $\varphi = 30°$. Solid lines: measured. Crosses: retrieved from the irregularly spaced NF data through the SVD-based technique.*

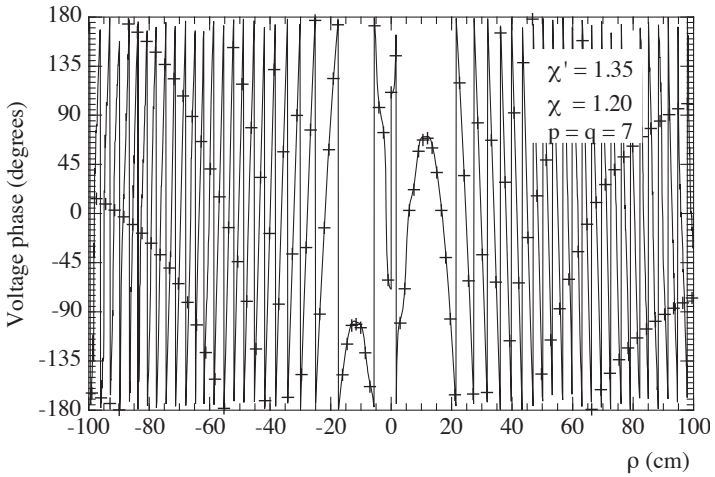

Fig. 6. *Phase of V_φ along the radial line at $\varphi = 30°$. Solid line: measured. Crosses: retrieved from the irregularly spaced NF data through the SVD-based technique.*

spatial bandwidth are removed owing to the low pass filtering characteristics of the OSI functions. In order to assess the overall effectiveness of the SVD-based approach, the E- and H-plane FF patterns retrieved from the nonuniformly spaced NF data are compared in Figs. 7 and 8 with those (references) attained via a cylindrical NF scanning system at the UNISA Antenna Characterization Lab. As can be seen, also the FF reconstructions are in good agreement, notwithstanding the reference FF patterns have been attained by applying a different NF scanning technique and the significant amount of the positioning errors affecting the NF data. The FF patterns directly reconstructed from the uncorrected nonuniform plane-polar NF data are shown in the same figures for sake of comparison. As can be clearly seen, the reconstructions are heavily compromised, thus further validating the effectiveness of the SVD technique in correcting even large known positioning errors. Note that the uniform samples reconstruction process has taken a CPU time of

about 25 seconds on a PC equipped with an Intel Core 2 Duo @ 3.33 GHz. The interested reader can find in [31] another set of experimental results assessing the effectiveness of the SVD-based approach and relevant to a different AUT.

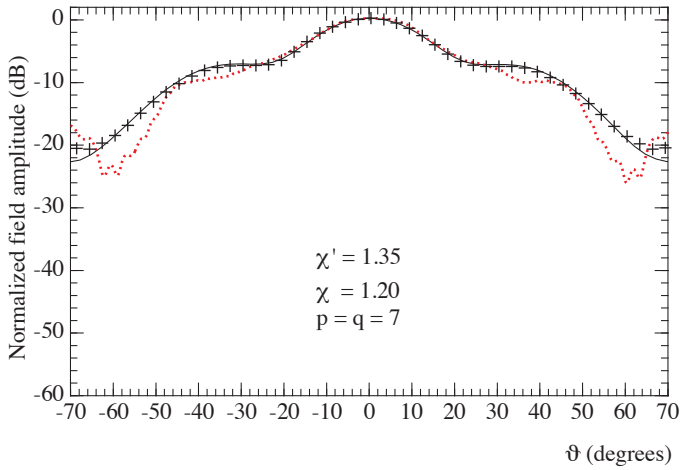

***Fig.** 7. E-plane pattern. Solid line: reference. Crosses: retrieved from the irregularly spaced NF data. Dashed line: directly retrieved from the uncorrected nonuniform NF data.*

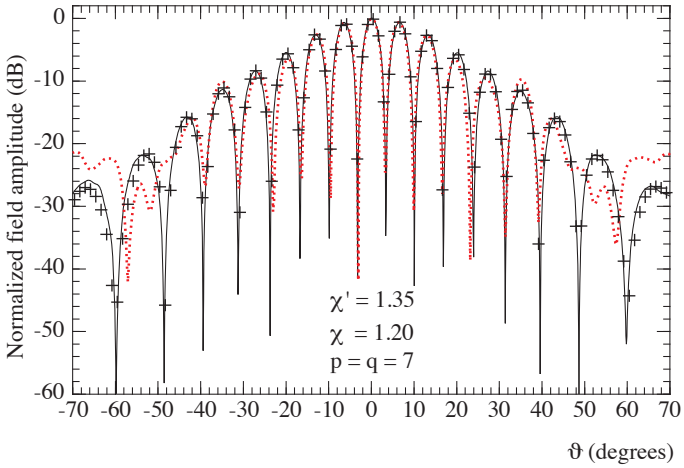

***Fig.** 8. H-plane pattern. Solid line: reference. Crosses: retrieved from the irregularly spaced NF data. Dashed line: directly retrieved from the uncorrected nonuniform NF data.*

The second set of results (from Fig. 9 to Fig. 12) refers to the case of nonuniform sampling points which do not lie on rings and, accordingly, the iterative technique has been applied. The nonuniform samples have been acquired in such a way that the displacements in ξ and φ between the position of each nonuniform sample and the related uniform one are random variables uniformly distributed in $[-\Delta\xi/3, \Delta\xi/3]$ and $[-\Delta\varphi_n/3, \Delta\varphi_n/3]$. The reconstructions of the amplitude and phase of V_ρ on the radial line at $\varphi = 90°$, obtained by using 10 iterations (enough to ensure the convergence of the algorithm with very low errors [26,

28]), are reported in Figs. 9 and 10, respectively. At last, the overall effectiveness of the iterative technique is confirmed by the E-plane and H-plane pattern reconstructions shown in Figs. 11 and 12. For completeness, the reconstructions obtained without using the iterative approach are also shown in the same figures. Note that the uniform samples reconstruction process has now taken a CPU time of about 1.74 seconds. A more complete set of experimental results relevant to the iterative technique can be found in [32].

It is noteworthy to compare the number of the nonuniform NF data acquired in both considered sets (1 675) with that (33 581) needed by the plane-polar scanning techniques [7-9] and with the one (21 609) required by the standard NF–FF transformation with plane-rectangular scan [6].

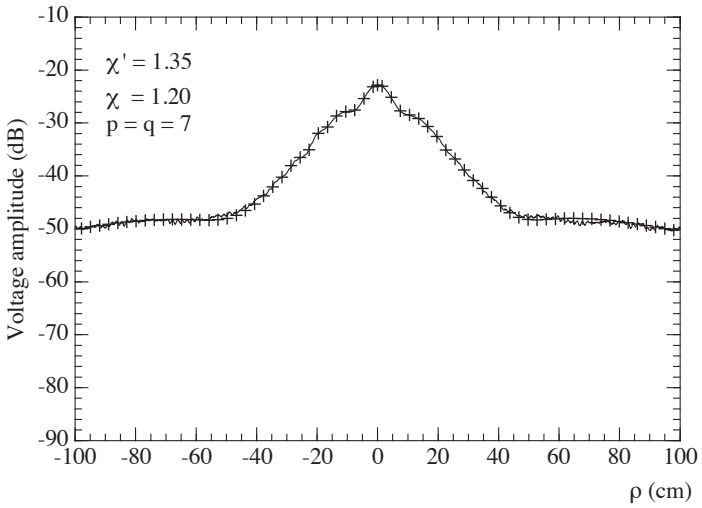

***Fig.** 9. Amplitude of V_ρ along the radial line at $\varphi = 90°$. Solid line: measured. Crosses: retrieved from the irregularly spaced NF data through the iterative algorithm.*

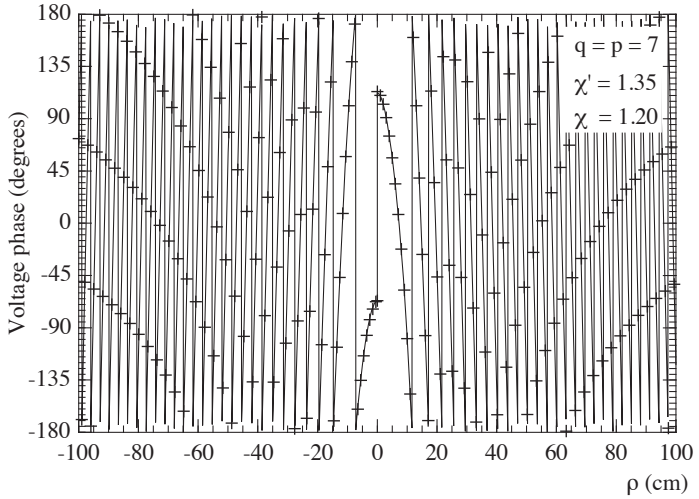

***Fig.** 10. Phase of V_ρ along the radial line at $\varphi = 90°$. Solid line: measured. Crosses: retrieved from the irregularly spaced NF data through the iterative algorithm.*

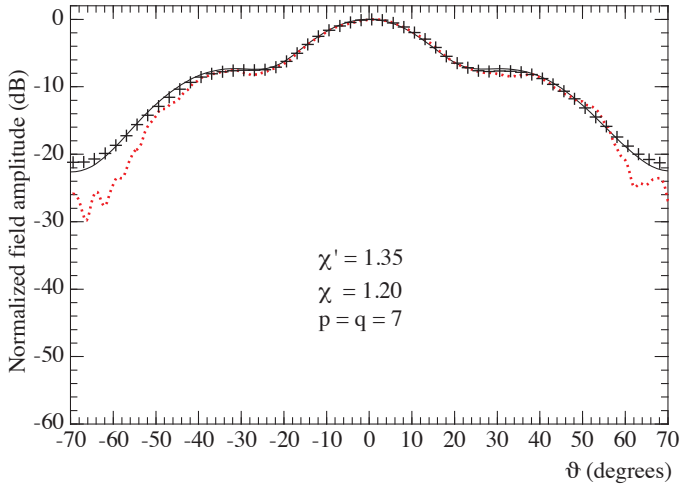

***Fig.** 11. E-plane pattern. Solid line: reference. Crosses: retrieved from the irregularly spaced NF data. Dashed line: directly retrieved from the uncorrected nonuniform NF data.*

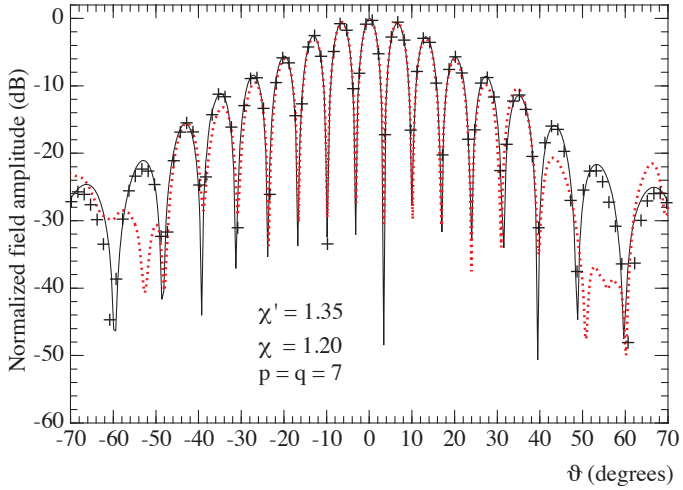

***Fig.** 12. H-plane pattern. Solid line: reference. Crosses: retrieved from the irregularly spaced NF data. Dashed line: directly retrieved from the uncorrected nonuniform NF data.*

5. Conclusion

Two efficient procedures for correcting known positioning errors affecting the NF data in a plane-polar scanning facility have been developed. Their effectiveness has been experimentally assessed by the very good NF and FF reconstructions obtained, in spite of the considered large and pessimistic positioning errors, when using the proposed techniques and by the deteriorated FF patterns resulting when they are not applied.

6. References

[1] Yaghjian, A.D.: 'An overview of near-field antenna measurements', *IEEE Trans. Antennas Propag.,* 1986, **AP-34**, (1), pp. 30-45

[2] Gillespie, E.S. (Ed.): 'Special Issue on near-field scanning techniques', *IEEE Trans. Antennas Propag.,* 1988, **36**, (6), pp. 727-901

[3] Francis, M.H., Wittmann, R.C.: 'Near-field scanning measurements: theory and practice', in Balanis, C.A. (Ed.): 'Modern Antenna Handbook', (John Wiley & Sons, Inc., Hoboken, NJ, 2008)

[4] Francis, M.H. (Ed.): 'IEEE Recommended Practice for Near-Field Antenna Measurements', IEEE Standard 1720-2012.

[5] C. Gennarelli, A. Capozzoli, L. Foged, *et al.* (Eds.): 'Special Issue on recent advances in near-field to far-field transformation techniques', *Int. Jour. Antennas Propag.*, 2012, article ID 243203

[6] Joy, E.B., Leach, W.M., Jr., Rodrigue, G. P., Paris, D.T.: 'Application of probe-compensated near-field measurements', *IEEE Trans. Antennas Propag.,* 1978, **AP-26**, (3), pp. 379-389

[7] Rahmat-Samii, Y., Galindo Israel, V., Mittra, R.: 'A plane-polar approach for far-field construction from near-field measurements', *IEEE Trans. Antennas Propag.,* 1980, **AP-28**, (2), pp. 216-230

[8] Rahmat-Samii, Y., Gatti, M.S.: 'Far-field patterns of spaceborne antennas from plane-polar near-field measurements', *IEEE Trans. Antennas Propag.,* 1985, **AP-33**, (6), pp. 638-648

[9] Gatti, M.S., Rahmat-Samii, Y.: 'FFT applications to plane-polar near-field antenna measurements', *IEEE Trans. Antennas Propag.,* 1988, **36**, (6), pp. 781-791

[10] Bucci, O.M., Gennarelli, C., Savarese, C.: 'Fast and accurate near-field–far-field transformation by sampling interpolation of plane-polar measurements', *IEEE Trans. Antennas Propag.*, 1991, **39**, (1), pp. 48-55

[11] Yaghjian, A.D.: 'Antenna coupling and near-field sampling in plane-polar coordinates', *IEEE Trans. Antennas Propag.,* 1992, **40**, (3), pp. 304-312

[12] Yaghjian, A.D., Woodworth, M.B.: 'Sampling in plane-polar coordinates', *IEEE Trans. Antennas Propag.,* 1996, **44**, (5), pp. 696-700

[13] Bucci, O.M., Gennarelli, C., Riccio, G., Savarese, C.: 'Near-field–far-field transformation from nonredundant plane-polar data: effective modellings of the source', *IEE Proc. Microw. Antennas Propag.*, 1998, **145**, (1), pp. 33-38

[14] D'Agostino, F., Ferrara, F., Gennarelli, C., et al.: 'An efficient NF-FF transformation technique with plane-polar scanning: experimental assessments'. Proc. of LAPC 2014, Loughborough, UK, November 2014, pp. 231-235

[15] Bucci, O.M., Gennarelli, C., Riccio, G., *et al.*: 'NF–FF transformation with plane-polar scanning: ellipsoidal modelling of the antenna', *Automatika*, 2000, **41**, (3-4), pp. 159-164

[16] D'Agostino, F., Ferrara, F., Gennarelli, C., *et al.*: 'Far-field pattern reconstruction from a nonredundant plane-polar near-field sampling arrangement: experimental testing', *IEEE Antennas Wirel. Propag. Lett.*, 2016, **15**, pp. 1345-1348

[17] Bucci, O.M., Franceschetti, G.: 'On the spatial bandwidth of scattered fields', *IEEE Trans. Antennas Propag.,* 1987, **AP-35**, (12), pp. 1445-1455

[18] Bucci, O.M., Gennarelli, C., Savarese, C.: 'Representation of electromagnetic fields over arbitrary surfaces by a finite and non redundant number of samples', *IEEE Trans. Antennas Propag.,* 1998, **46**, (3), pp. 351-359

[19] Bucci, O.M., Gennarelli, C.: 'Application of nonredundant sampling representations of electromagnetic fields to NF-FF transformation techniques', *Int. Jour. Antennas Propag.*, 2012, article ID 319856, 14 pages

[20] Dutt, A., Rokhlin, V.: 'Fast Fourier transforms for non equispaced data', *Proc. SIAM Jour. Scient. Comp.,* 1993, **14**, (6), pp. 1369–1393

[21] Wittmann, R.C., Alpert, B.K., Francis, M.H.: 'Near-field antenna measurements using nonideal measurement locations', *IEEE Trans. Antennas Propag.,* 1998, **46**, (5), pp. 716-722

[22] Bucci, O.M., Gennarelli, C., Savarese, C.: 'Interpolation of electromagnetic radiated fields over a plane from nonuniform samples', *IEEE Trans. Antennas Propag.,* 1993, **41**, (11), pp. 1501–1508

[23] Bucci, O.M., Gennarelli, C., Riccio, G., Savarese, C.: 'Electromagnetic fields interpolation from nonuniform samples over spherical and cylindrical surfaces', *IEE Proc. Microw. Antennas Propag.*, 1994, **141**, (2), pp. 77–84

[24] Ferrara, F., Gennarelli, C., Riccio, G., Savarese, C.: 'Far field reconstruction from nonuniform plane-polar data: a SVD based approach', *Electromagnetics,* 2003, **23**, (5), pp. 417–429

[25] Ferrara, F., Gennarelli, C., Riccio, G., Savarese, C.: 'NF–FF transformation with cylindrical scanning from nonuniformly distributed data', *Microw. Opt. Technol. Lett*., 2003, **39**, (1), pp. 4-8

[26] D'Agostino, F., Ferrara, F., Gennarelli, C., *et al.*: 'On the compensation of probe positioning errors when using a nonredundant cylindrical NF–FF transformation', *Prog. Electromagn. Res. B*, 2010, **20***,* pp. 321–335

[27] Ferrara, F., Gennarelli, C., Guerriero, R., Migliozzi, M.: 'Experimental validation of the NF–FF transformation with cylindrical scan from nonuniformly distributed data', *Microw. Opt. Technol. Lett*., 2011, **53**, (4), pp. 915-920

[28] D'Agostino, F., Ferrara, F., Gennarelli, C., *et al.*: 'Two techniques for compensating the probe positioning errors in the spherical NF–FF transformation for elongated antennas', *The Open Electr. & Electron. Eng. Jour.,* 2011, **5**, pp. 29–36

[29] D'Agostino, F., Ferrara, F., Gennarelli, C., *et al.*: 'An effective NF-FF transformation technique with planar spiral scanning tailored for quasi-planar antennas', *IEEE Trans. Antennas Propag.,* 2008, **56**, (9), pp. 2981-2987

[30] Yaghjian, A.D.: 'Approximate formulas for the far field and gain of open-ended rectangular waveguide', *IEEE Trans. Antennas Propag.*, 1984, **AP-32**, (4), pp. 378-384

[31] D'Agostino, F., Ferrara, F., Gennarelli, C., *et al.*: 'Far field reconstruction from positioning errors affected plane-polar measurements: a SVD approach'. Proc. of ICEAA 2015, Turin, Italy, September 2015, pp. 183-186

[32] D'Agostino, F., Ferrara, F., Gennarelli, C., *et al.*: 'An efficient iterative procedure to correct the positioning errors in the plane-polar scanning'. Proc. of LAPC 2015, Loughborough, UK, November 2015, pp. 335-339